Heterologous Vaccination with SARS-CoV-2 Spike saRNA Prime followed by DNA Dual-Antigen Boost Induces Robust Antibody and T-Cell Immunogenicity against both Wild Type and Delta Spike as well as Nucleocapsid Antigens

Adrian Rice[1φ], Mohit Verma[1φ], Emily Voigt[2φ], Peter Battisti[2], Sam Beaver[2], Sierra Reed[2], Kyle Dinkins[1], Shivani Mody[1], Lise Zakin[1], Peter Sieling[1], Shiho Tanaka[1], Brett Morimoto[1], Wendy Higashide[1], C. Anders Olson[1], Elizabeth Gabitzsch[1], Jeffrey T. Safrit[1], Patricia Spilman[1], Corey Casper[2,3], Patrick Soon-Shiong[1]*

[1]ImmunityBio, Inc., 9920 Jefferson Blvd., Culver City, CA, 90232 USA

[2]Infectious Disease Research Institute (IDRI), 1616 Eastlake Ave. East, Seattle, WA, 98102, USA

[3]Departments of Medicine and Global Health, University of Washington, 1959 Pacific Street NE, Seattle, WA, 98195, USA

*Corresponding author Patrick Soon-Shiong: Patrick@Nantworks.com

[φ]These authors contributed equally

ABSTRACT

We assessed if immune responses are enhanced in CD-1 mice by heterologous vaccination with two different nucleic acid-based COVID-19 vaccines: a next-generation human adenovirus serotype 5 (hAd5)-vectored dual-antigen spike (S) and nucleocapsid (N) vaccine (AdS+N) and a self-amplifying and -adjuvanted S RNA vaccine (SASA S) delivered by a nanostructured lipid carrier. The AdS+N vaccine encodes S modified with a fusion motif to increase cell-surface expression. The N antigen is modified with an Enhanced T-cell Stimulation Domain (N-ETSD) to direct N to the endosomal/lysosomal compartment to increase the potential for MHC class I and II stimulation. The S sequence in the SASA S vaccine comprises the D614G mutation, two prolines to stabilize S in the prefusion conformation, and 3 glutamines in the furin cleavage region to increase cross-reactivity across variants. CD-1 mice received vaccination by prime > boost homologous and heterologous combinations. Humoral responses to S were the highest with any regimen including the SASA S vaccine, and IgG against wild type S1 and Delta (B.1.617.2) variant S1 was generated at similar levels. An AdS+N boost of an SASA S prime enhanced both CD4+ and CD8+ T-cell responses to both S wild type and S Delta peptides relative to all other vaccine regimens. Sera from mice receiving SASA S homologous or heterologous vaccination were found to be highly neutralizing of all pseudovirus tested: Wuhan, Delta, and Beta strain pseudoviruses. The findings here support the clinical testing of heterologous vaccination by an SASA S > AdS+N regimen to provide increased protection against COVID-19 and SARS-CoV-2 variants.

47 **INTRODUCTION**

48 Impressive efforts of the scientific and pharmaceutical community have resulted in the design,
49 testing and successful deployment of several COVID-19 vaccines that have shown high levels of
50 efficacy.[1-5] Nonetheless, SARS-CoV-2 viral variants have continued to emerge and spread
51 throughout the globe, particularly in areas where vaccination rates are low or vaccines are
52 unavailable.

53 To address the need for a vaccine regimen that would be highly efficacious against
54 predominating and emerging variants that may be made available in currently underserved areas
55 and nations, and leverages the resilience of cell-mediated immunity against variants, we previously
56 developed a next-generation human adenovirus serotype 5 (hAd5)-vectored dual-antigen spike (S)
57 plus nucleocapsid (N) vaccine (AdS+N). [6,7] This vaccine encoding Wuhan strain or 'wild type'
58 (wt) SARS-CoV-2 S modified with a fusion sequence (S-Fusion) to enhance cell-surface
59 expression [6,7] as well as N modified with an Enhanced T-cell Stimulation Domain (N-ETSD) [8] to
60 increase the potential for MHC class I and II stimulation [9-11] has been shown to elicit humoral and
61 T-cell responses in mice, [7] non-human primates (NHP), [6] and participants in Phase 1b trials. [8] The
62 Ad5S+N vaccine given as a subcutaneous (SC) prime with two oral boosts protected NHP from
63 SARS-CoV-2 infection [6] and a single prime vaccination of clinical trial participants generated T-
64 cell responses that were sustained against a series of variant S peptide sequences, including those
65 for the B.1.351, B.1.1.7, P.1, and B.1.426 variants. [8]

66 Despite the promising findings with the AdS+N vaccine candidate, we wish to continue to
67 investigate vaccine regimens with the potential to maximize immune responses – both humoral
68 and cellular. One such approach is by heterologous vaccination utilizing two nucleic acid-based
69 vaccines: ImmunityBio's hAd5 vectored DNA vaccine and the Infectious Disease Research

70 Institute's (IDRI's) RNA-based vaccine. [12] Heterologous vaccination using vaccine constructs
71 expressing the same or different antigens vectored by different platforms, specifically
72 combinations of RNA- and adenovirus-based vaccines has previously been reported to
73 significantly increase immune responses. [13,14]

74 To assess the potential for enhanced immune responses by heterologous vaccination, we tested
75 prime > boost combinations of the AdS+N vaccine with a self-amplifying and self-adjuvanted
76 S(wt) RNA-based vaccine (SASA S) delivered in a nanostructured lipid carrier (NLC). [15,16] The
77 NLC stabilizes the self-amplifying RNA [17-19] and delivers it to cells wherein it is amplified and the
78 S protein expressed. The S sequence in the SASA S vaccine comprises a codon-optimized
79 sequence with the D614G mutation [20] that increases SARS-CoV-2 susceptibility to neutralization,
80 [21] a diproline modification to stabilize S in the pre-fusion conformation that increases antigenicity,
81 [22] and a tri-glutamine (3Q) repeat in the furin cleavage region to broaden immune responses against
82 variants. [23] Preclinical studies of the SASA S vaccine have demonstrated the vaccine elicited
83 vigorous antigen-specific and virus-neutralizing IgG and polyfunctional CD4+ and CD8+ T-cell
84 responses after both a prime and boost in C57Bl/6 mice.

85 In this work, the two aforementioned vaccines were tested by homologous prime > boost
86 delivery of each as compared to heterologous delivery regimens with an alternating order: AdS+N
87 > SASA S and SASA S > AdS+N. The findings reported here support our hypothesis that
88 heterologous vaccination with the SASA S and AdS+N vaccines would enhance immune
89 responses, particularly T-cell responses.

90 Both CD4+ and CD8+ T-cell responses were enhanced by heterologous vaccination, with
91 CD4+ interferon-γ (IFN-γ) production in response to both S(wt) peptides being higher with the
92 SASA S prime > AdS+N boost combination as compared to all other groups. Notably, CD4+ and

93 CD8+ T cells were equally responsive to S(wt) and S(Delta) peptides and responses of T cells
94 from SASA S > AdS+N to S(Delta) were also the highest of the groups.
95 Findings were similar for unselected T cells in ELISpot analyses, which again revealed the
96 SASA S > AdS+N combination resulted in significantly higher IFN-γ secretion by T cells in
97 response to both S(wt) peptides than all other groups.
98 We further demonstrate that all combinations that included the SASA S vaccine elicited the
99 greatest anti-full length (FL) S wild type (wt), anti-S1(wt) and – importantly- anti-Delta variant
100 (B.1.617.2) S1 IgG responses. Regimens comprising the SASA S vaccine also generated sera that
101 showed high and similar capability to neutralize Wuhan, Delta, and Beta strain pseudovirus.
102 As expected, anti-N IgG antibodies and T-cell responses to N peptides were seen only for
103 vaccine combinations that delivered the N antigen and were very similar among groups receiving
104 the AdS+N vaccine in any order.

105 **METHODS**

106 *The hAd5 [E1-, E2b-, E3-] platform and constructs*

107 For studies here, the next generation hAd5 [E1-, E2b-, E3-] vector was used to create viral
108 vaccine candidate constructs. [6] This hAd5 [E1-, E2b-, E3-] vector is primarily distinguished from
109 other first-generation [E1-, E3-] recombinant Ad5 platforms [24,25] by having additional deletions in
110 the early gene 2b (E2b) region that remove the expression of the viral DNA polymerase (pol) and
111 in pre terminal protein (pTP) genes, and its propagation in the E.C7 human cell line. [26-29]
112 The AdS+N vaccine expresses a wild type spike (S) sequence [accession number
113 YP009724390] modified with a proprietary 'fusion' linker peptide sequence as well as a wild type
114 nucleocapsid (N) sequence [accession number YP009724397] with an Enhanced T-cell

115 Stimulation Domain (ETSD) signal sequence to direct translated N to the endosomal/lysosomal
116 pathway [8] as described in Gabitzsch *et al*., 2021. [6]

117 The SASA S vaccine comprises an saRNA replicon composed of an 11.7 kb construct
118 expressing the SARS-CoV-2 Spike protein, along with the non-structural proteins 1-4 derived from
119 the Venezuelan equine encephalitis virus (VEEV) vaccine strain TC-83. The Spike RNA sequence
120 is codon-optimized and expresses a protein with the native sequence of the original Wuhan strain
121 plus the dominant D614G mutation, with the prefusion conformation-stabilizing diproline (pp)
122 mutation (consistent with other vaccine antigens) and replacement of the furin cleavage site RRAR
123 sequence with a QQAQ sequence, as shown in Figure 1.

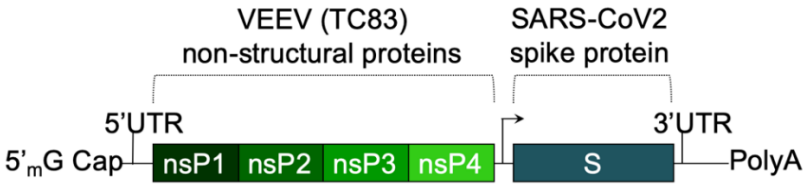

124
125
126 **Fig. 1** *The saRNA(D614G)-2P-3Q-NLC (SASA S) vaccine*. The SASA S vaccine comprises an
127 saRNA replicon backbone consisting of the non-structural protein (nsPs) 1-4 derived from the
128 Venezuelan equine encephalitis virus (VEEV) vaccine strain TC-83 and an independent open
129 reading frame under the control of a subgenomic promoter sequence that contains Wuhan sequence
130 S with a diproline (pp) mutation and a QQAQ furin cleavage site sequence.
131
132 The RNA is generated by T7 promoter-mediated *in vitro* transcription using a linearized DNA
133 template. *In vitro* transcription is performed using an in house-optimized protocol [12,30,31] using T7
134 polymerase, RNase inhibitor, and pyrophosphatase enzymes. DNA plasmid is digested with
135 DNase I and the RNA is capped by vaccinia capping enzyme, guanosine triphosphate, and S-
136 adenosyl-methionine. RNA is then purified from the transcription and capping reaction
137 components by chromatography using a CaptoCore 700 resin (GE Healthcare) followed by
138 diafiltration and concentration using tangential flow filtration into 10 mM Tris buffer. The RNA
139 material is terminally filtered with a 0.22 µm polyethersulfone filter and stored at -80ºC until use.

140 The RNA-stabilizing nanostructured lipid carrier (NLC) is comprised of particles with a
141 hybrid liquid and solid oil core, which provides colloidal stability [32] Non-ionic hydrophobic and
142 hydrophilic surfactants help maintain a stable nanoparticle droplet, while a cationic lipid provides
143 the positive charge for electrostatic binding of RNA. That binding on the surface of the
144 nanoparticles protects RNA from degradation by RNases and allowing delivery to cells that will
145 express the S antigen.

146 NLC is manufactured by mixing the lipids in an oil phase, dissolving the Tween 80 in citrate
147 buffer aqueous phase, and homogenizing the two phases by micro-fluidization. The resulting
148 emulsion is sterile-filtered and vialed, and reconstituted in an appropriate buffer before use.

149 *Murine immunization and blood/tissue collection*

150 The design of vaccination study performed using CD-1 mice is shown in Figure 2.

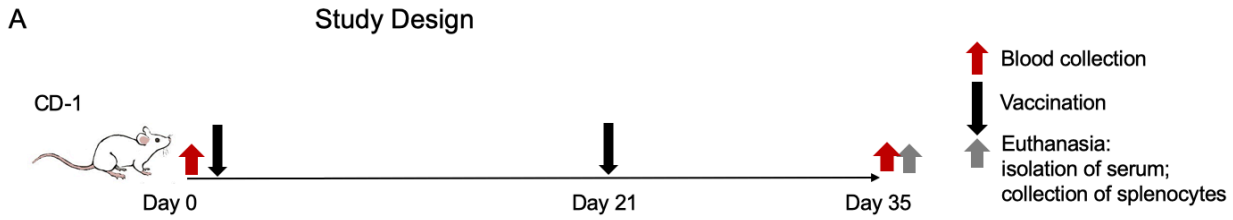

B

N #	Prime	Route (Dose)	Boost Dose	Route (Dose)	Code
4	Untreated		untreated		UnTx
7	hAd5 S-Fusion+N-ETSD	$1x10^{10}$ VP (SC)	hAd5 S-Fusion+N-ETSD	$1x10^{10}$ VP (SC)	AdS+N > AdS+N
6	saRNA(D614G-2P-3Q)-NLC	10 µg (IM)	saRNA(D614G-2P-3Q)-NLC	10 µg (IM)	SASA S > SASA S
7	hAd5 S-Fusion+N-ETSD	$1x10^{10}$ VP (SC)	saRNA(D614G-2P-3Q)-NLC	10 µg (IM)	AdS+N > SASA S
7	saRNA(D614G-2P-3Q)-NLC	10 µg (IM)	hAd5 S-Fusion+N-ETSD	$1x10^{10}$ VP (SC)	SASA S > AdS+N

151
152 **Fig. 2** *Study design and vaccine description*. (A) CD-1 mice received prime vaccination on Day 0
153 after blood collection and the boost on Day 21; mice were euthanized and tissues/blood collected
154 on Day 35. (B) The various combinations of prime > boost are shown, including: AdS+N
155 homologous; saRNA(D614G-2P-3Q)-NLC (SASA S) homologous; Ad5S+N prime, SASA S
156 boost; and SASA S prime, AdS+N boost. Untreated mice were used as controls. All were n = 7
157 with the exception of untreated n = 4 and SASA S homologous n = 6. The color code for each
158 group is shown.
159

160 All *in vivo* experiments described were carried out in strict accordance with good animal
161 practice according to NIH recommendations. All procedures for animal use were approved by the
162 IACUC Committee at Omeros, Inc. (Seattle, WA, USA) and under an approved protocol.

163 CD-1 female mice (Charles River Laboratories) 6-8 weeks of age were used for
164 immunological studies performed at the vivarium facilities of Omeros Inc. (Seattle, WA). The
165 adenovirus-vectored vaccines were administered by subcutaneous (SC) injections at the indicated
166 doses in 50 μL ARM buffer (20 mM Tris pH 8.0, 25 mM NaCl, with 2.5% glycerol). The SASA
167 S vaccine was administered intramuscularly (IM) in 10% sucrose 5 mM sodium citrate solution at
168 a dose of 10 μg.

169 On the final day of each study, blood was collected via the submandibular vein from
170 isoflurane-anesthetized mice for isolation of sera using a microtainer tube and then mice were
171 euthanized for collection of spleens. Spleens were removed from each mouse and placed in 5 mL
172 of sterile media (RPMI/HEPES/Pen/Strep/10% FBS). Splenocytes were isolated [33] within 2 hours
173 of collection and used fresh or frozen for later analysis.

174 *Intracellular cytokine stimulation (ICS)*

175 ICS assays were performed using 10^6 live splenocytes per well in 96-well U-bottom plates.
176 Splenocytes in RPMI media supplemented with 10% FBS were stimulated by the addition of pools
177 of overlapping peptides spanning the SARS-CoV-2 S protein (both wild type, wt, or Delta
178 sequence) or N antigens at 2 μg/mL/peptide for 6 h at 37°C in 5% CO_2, with protein transport
179 inhibitor, GolgiStop (BD) added two hours after initiation of incubation. The S peptide pool (wild
180 type, JPT Cat #PM-WCPV-S-1; Delta, JPT cat# PM-SARS2-SMUT06-1) is a total of 315 spike
181 peptides split into two pools, S1 and S2, comprised of 158 and 157 peptides each. The N peptide
182 pool (JPT; Cat # PM-WCPV-NCAP-1) was also used to stimulate cells. A SIV-Nef peptide pool

183 (BEI Resources) was used as an off-target negative control. Stimulated splenocytes were then
184 stained with a fixable cell viability stain (eBioscience™ Fixable Viability Dye eFluor™ 506 Cat#
185 65-0866-14) followed by the lymphocyte surface markers CD8β and CD4, fixed with CytoFix
186 (BD), permeabilized, and stained for intracellular accumulation of IFN-γ, TNF-α and IL-2.
187 Fluorescent-conjugated anti-mouse antibodies used for labeling included CD8β antibody (clone
188 H35-17.2, ThermoFisher), CD4 (clone RM4-5, BD), IFN-γ (clone XMG1.2, BD), TNF-α (clone
189 MP6-XT22, BD) and IL-2 (clone JES6-5H4; BD), and staining was performed in the presence of
190 unlabeled anti-CD16/CD32 antibody (clone 2.4G2; BD). Flow cytometry was performed using a
191 Beckman-Coulter Cytoflex S flow cytometer and analyzed using Flowjo Software.

192 *ELISpot assay*

193 ELISpot assays were used to detect cytokines secreted by splenocytes from inoculated mice.
194 Fresh splenocytes were used on the same day as harvest, and cryopreserved splenocytes containing
195 lymphocytes were used the day of thawing. The cells (2-4 x 10^5 cells per well of a 96-well plate)
196 were added to the ELISpot plate containing an immobilized primary antibody to either IFN-γ or
197 IL-4 (BD Cat# 551881 and BD Cat# 551878, respectively), and were exposed to various stimuli
198 (e.g. control peptides SIV and ConA, S-WT and N peptides pools – see catalog numbers above) at
199 a concentration of 1-2 μg/mL peptide pools for 36-40 hours. After aspiration and washing to
200 remove cells and media, extracellular cytokine was detected by a biotin-conjugated secondary
201 antibody to cytokine conjugated to biotin (BD), followed by a streptavidin/horseradish peroxidase
202 conjugate was used detect the biotin-conjugated secondary antibody. The number of spots per well,
203 or per 2-4 x 10^5 cells, was counted using an ELISpot plate reader. Quantification of Th1/Th2 bias
204 was calculated by dividing the IFN-γ spot forming cells (SFC) per million splenocytes with the
205 IL-4 SFC per million splenocytes for each animal.

206 *ELISA for detection of antibodies*

207 For IgG antibody detection in inoculated mouse sera and lung homogenates, ELISAs for
208 spike-binding (including S1 Delta) and nucleocapsid-binding antibodies and IgG subclasses
209 (IgG1, IgG2a, IgG2b, and IgG3) were used. A microtiter plate was coated overnight with 100 ng
210 of either purified recombinant SARS-CoV-2 S-FTD (FL S with fibritin trimerization domain,
211 constructed and purified in-house by ImmunityBio), purified recombinant Spike S1 domain
212 (S1(wt)) (Sino; Cat # 40591-V08B1), purified recombinant Delta variant Spike S1 domain
213 (S1(Delta)) (Sino; Cat # 40591-V08H23), or purified recombinant SARS-CoV-2 nucleocapsid (N)
214 protein (Sino; Cat # 40588-V08B) in 100 µL of coating buffer (0.05 M Carbonate Buffer, pH 9.6).
215 The wells were washed three times with 250 µL PBS containing 1% Tween 20 (PBST) to remove
216 unbound protein and the plate was blocked for 60 minutes at room temperature with 250 µL PBST.
217 After blocking, the wells were washed with PBST, 100 µL of either diluted serum or diluted lung
218 homogenate samples was added to each well, and samples incubated for 60 minutes at room
219 temperature. After incubation, the wells were washed with PBST and 100 µL of a 1/5000 dilution
220 of anti-mouse IgG HRP (GE Health Care; Cat # NA9310V), anti-mouse IgG_1 HRP (Sigma; Cat #
221 SAB3701171), anti-mouse IgG_{2a} HRP (Sigma; Cat # SAB3701178), anti-mouse IgG_{2b} HRP
222 (Sigma; catalog# SAB3701185), anti-mouse IgG_3 HRP conjugated antibody (Sigma; Cat #
223 SAB3701192), or anti-mouse IgA HRP conjugated antibody (Sigma; Cat # A4789) was added to
224 wells. For positive controls, 100 µL of a 1/5000 dilution of rabbit anti-N IgG Ab or 100 µL of a
225 1/25 dilution of mouse anti-S serum (from mice immunized with purified S antigen in adjuvant)
226 were added to appropriate wells. After incubation at room temperature for 1 hour, the wells were
227 washed with PBS-T and incubated with 200 µL o-phenylenediamine-dihydrochloride (OPD
228 substrate (Thermo Scientific Cat # A34006) until appropriate color development. The color

229 reaction was stopped with addition of 50 μL 10% phosphoric acid solution (Fisher Cat # A260-
230 500) in water and the absorbance at 490 nm was determined using a microplate reader (SoftMax
231 Pro, Molecular Devices).

232 *Calculation of relative ng amounts of antibodies and the Th1/Th2 IgG subclass bias*

233 A standard curve of IgG for OD vs. ng mouse IgG was generated using purified mouse IgG
234 (Sigma Cat #15381; absorbance values were converted into mass equivalents for both anti-S and
235 anti-N antibodies. Using these values, we calculated the geometric mean value for S- and N-
236 specific IgG per milliliter of serum induced by vaccination. These values were also used to quantify
237 the Th1/Th2 bias for the humoral responses by dividing the sum total of Th1 biased antigen-
238 specific IgG subclasses (IgG2a, IgG2b and IgG3) with the total Th2 skewed IgG3, for each mouse.
239 For mice that lack anti-S and/or anti-N specific IgG responses, Th1/Th2 ratio was not calculated.
240 Conversely, some responses, particularly for anti-N responses in IgG2a and IgG2b (both Th1
241 biased subclasses), were above the limit of quantification with OD values higher than those
242 observed in the standard curve. These data points were reduced to values within the standard curve,
243 and thus will reflect a lower Th1/Th2 bias than would otherwise be reported.

244 *Endpoint titers*

245 Serial dilutions were prepared from each serum sample, with dilution factors ranging from
246 400 to 6,553,600 in 4-fold steps. These dilution series were characterized by whole IgG ELISA
247 assays against both recombinant S1(wt) and recombinant S1(Delta), as described above. Half
248 maximal response values (Ab_{50}) were calculated by non-linear least squares fit analysis on the
249 values for each dilution series against each recombinant S1 in GraphPad Prism. Serum samples
250 from mice without anti-S responses were removed Ab_{50}, μg IgG/mL sera, and endpoint titer
251 analyses and reported as N/D on the graphs. Endpoint titers were defined as the last dilution with

252 an absorbance value at least 3 standard deviations higher than the standard deviation of all readings
253 from serum of untreated animals (n = 32 total negative samples). Quantitative titration values (μg
254 IgG/mL sera) were calculated against a standard curve as described above.

255 *Pseudovirus neutralization assay*

256 SARS-CoV-2 pseudovirus neutralization assays were conducted on immunized mouse serum
257 samples using procedures adapted from Crawford *et al.,* 2020. [34] In brief, lentiviral pseudoviruses
258 expressing SARS-CoV-2 spike protein variants were prepared by co-transfecting HEK293 cells
259 (ATCC CRL-3216) with a plasmid containing a lentiviral backbone expressing luciferase and
260 ZsGreen (BEI Resources NR-52516), plasmids containing lentiviral helper genes (BEI Resources
261 NR-52517, NR-52518, NR-52519), and a delta19 cytoplasmic tail-truncated SARS-CoV-2 spike
262 protein expression plasmid (Wuhan strain, B.1.1.7, and B.1.351 spike variant plasmids were a gift
263 from Jesse Bloom of Fred Hutchinson Cancer Research Center; B.1.617.2 "delta" variant plasmid
264 a gift from Thomas Peacock of Imperial College London). Pseudovirus stocks were harvested from
265 the cell culture media after 72 hours of incubation at 37°C, 5% CO_2, filtered through a 0.2 μm
266 filter, and frozen until use.

267 Mouse serum samples were diluted 1:10 in media (Gibco DMEM + GlutaMAX + 10% FBS)
268 and then serially diluted 1:2 for 11 total dilutions, and incubated with polybrene (Sigma) and
269 pseudovirus for 1 hour at room temperature. Serum-virus mix was then added in duplicate to
270 seeded hACE2 expressing HEK293 cells (BEI Resources) and incubated at 37°C, 5% CO_2 for 72
271 hours. To determine 50% inhibitory concentration (IC50) values, plates were scanned on a high
272 content fluorescent imager (Molecular Devices ImageXpress Pico) for ZsGreen expression. Total
273 integrated intensity per well was used to calculate % pseudovirus inhibition noted in each well.

274 Neutralization curves were fit with a four-parameter sigmoidal curve which was used to calculate
275 IC50 values.

276 *Statistical analyses and graph generation*

277 All statistical analyses were performed and graphs generated used in figures were generated
278 using GraphPad Prism software. Statistical tests for each graph are described in the figure legends.
279 Statistical analyses of Endpoint Titer for anti-S1 IgG (Figure 4) was performed by assignment of
280 a value of 200 – one half the Level of Detection (LOD) of 400 – to the 4 animals with serum values
281 below the LOD.

282 **RESULTS**

283 **The SASA S vaccine enhanced generation of anti-S(wt) IgG**

284 Mice receiving the SASA S vaccine in any homologous or heterologous vaccination regimen
285 had the highest levels of anti-full length S(wt) (FL S) IgG2a and 2b as determined by OD at 490
286 nm in ELISA (Fig. 3A). As expected, only mice receiving the N antigen generated anti-N IgG
287 (also determined by OD at 490 nm in ELISA), which was similar for all groups receiving an N-
288 containing antigen (Fig. 3B) by AdS+ N homologous, prime, or boost vaccination. Determination
289 of the IgG1/IgG2a + IgG2b + IgG3 ratio using ng amounts calculated from the OD reading (see
290 *Methods*) revealed responses were highly T helper cell 1 (Th1)-biased, with all calculated values
291 being greater than one (Fig. 3C).

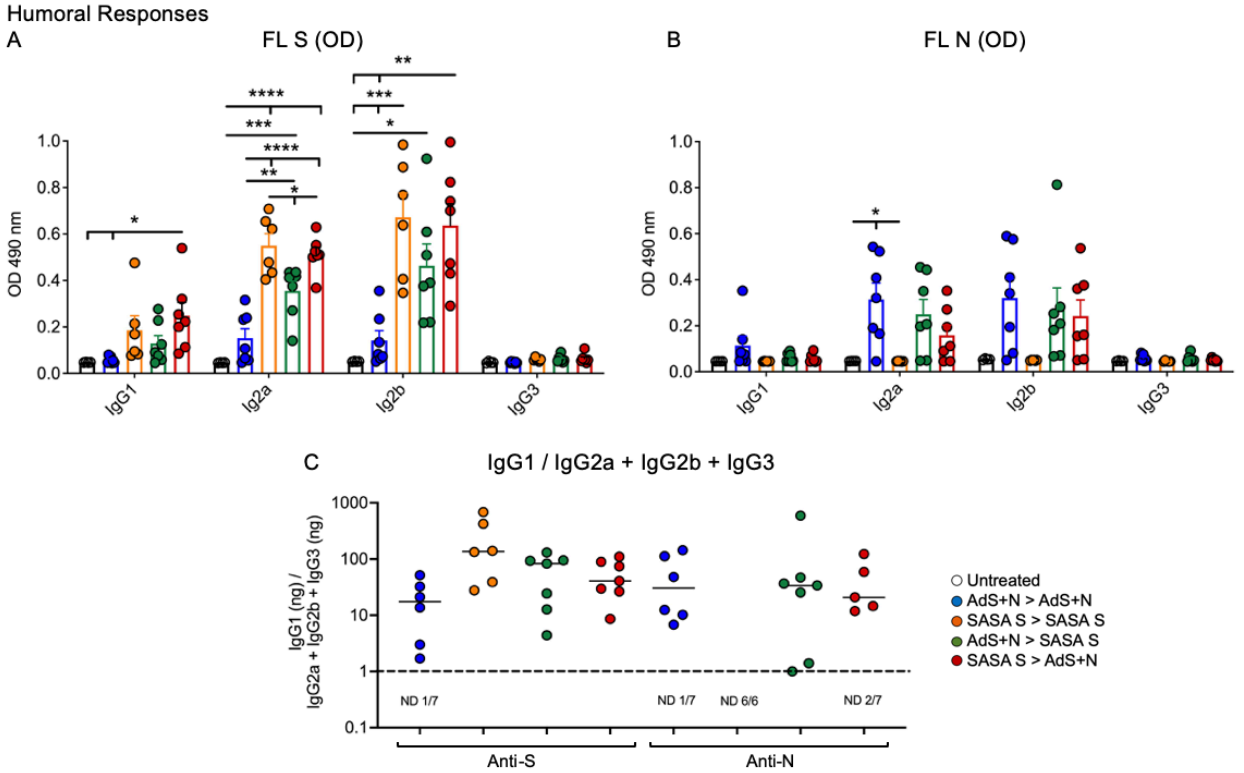

Fig. 3 *Anti-full length (FL) spike wild type (Swt) and -nucleocapsid (N) IgG antibody levels in sera show T helper cell 1 (Th1) bias*. (A) Levels of anti-FL Swt and (B) anti-N IgG1, IgG2a, IgG2b and IgG3 subtypes represented by OD at 490 nm from ELISA of sera are shown. Statistical analyses performed using one-way ANOVA and Tukey's post-hoc comparison of all groups to all other groups with the exception of comparison to the SASA S > group t SASA S hat did not receive an N antigen for anti-N IgG; where *$p \leq 0.05$, **$p < 0.01$, ***$p < 0.001$, and ****$p<0.0001$. (C) The IgG1/IgG2a+IgG2b+IgG3 ratio calculated using the ng equivalents for each is shown with a dashed line at 1. Values > 1 reflect Th1 bias. The number (n) of animals in which the ratio was not determined due to very low antibody levels is shown below the x-axis for each group. The homologous SASA S group did not receive an N antigen. Data graphed as the mean and SEM. The legend in C applies to all figure panels.

Humoral responses against wildtype and Delta S1 were similar in all SASA S groups

To assess serum antibody production specific for delta B.1.617.2 variant as compared to wild type S, an ELISAs were performed using either the wt or B.1.617.2 sequence S1 domain of S, which contains the RBD.

Vaccine regimens including the SASA S vaccine elicited the highest anti-S1(wt) and S1(Delta) responses as represented by the Ab_{50}, µg IgG/mL, and endpoint titers (Fig. 4A, B, and C, respectively). Four of seven AdS+N homologous vaccinated mice had serum IgG levels against

these antigens that were below the level of detection. Overall, the mean antibody titers for SASA S homologous and SASA S > AdS+N groups were highest. For Ab_{50} and µg IgG/mL (Fig. A and B) statistical comparison of the AdS+N group to other groups was not performed because of the presence of values below the LOD in the AdS+N group. For endpoint titer (Fig. 4C**),** the only significant difference was observed between AdS+N homologous versus SASA S homologous vaccination for anti-S1(delta) IgG, with the caveat that for this statistical analysis, serum values of 200 for those animals with IgG below the LOD of 400 were used.

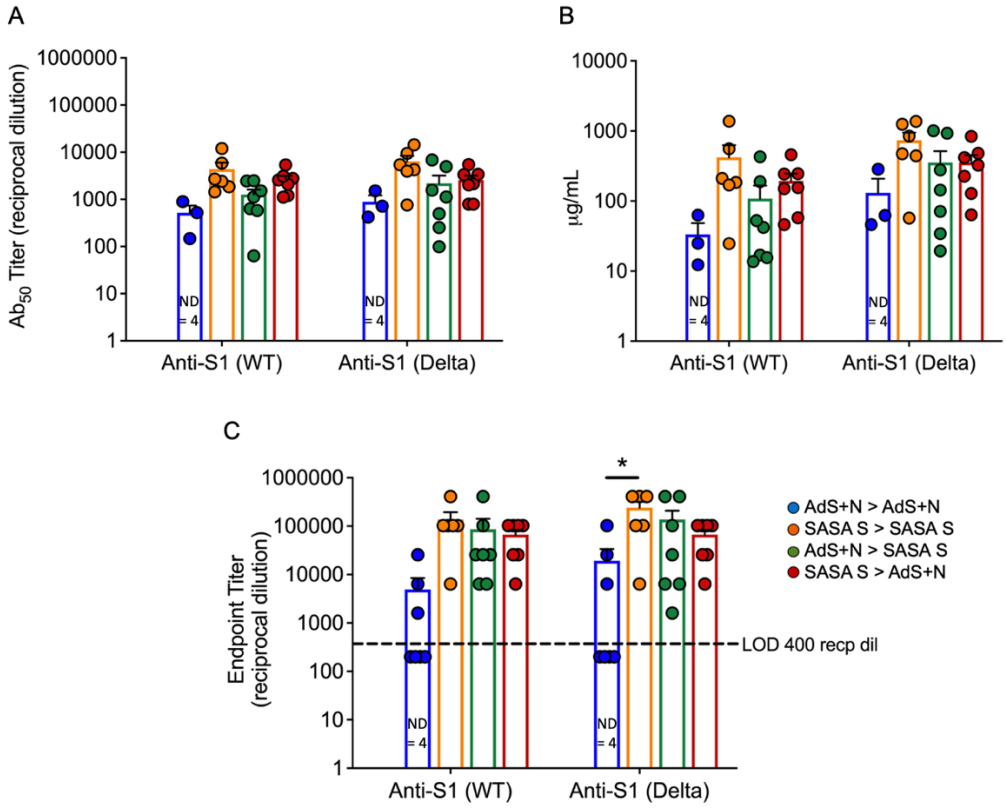

Fig. 4 *Wildtype and B.1.617.2 'Delta' S1-specific IgG endpoint titers*. Levels of anti-S1(wt) and -Delta S1 IgG are shown by (A) Ab_{50} reciprocal dilution, (B) µg/mL sera, and (C) endpoint titer reciprocal dilution. Values were below the level of detection in 4 of 7 AdS+N homologous group mice. Statistical analyses performed using one-way ANOVA and Tukey's post-hoc comparison of all groups for anti-S1 (WT) or -S1 (Delta) for (C) only where * $p = 0.0333$; sera without detectable levels of anti-S1 IgG were assigned a value of 200, one-half the Limit of Detection (LOD) of 400. Data graphed as the mean and SEM. The legend in C applies to all figure panels.

329 **An AdS+N boost after SASA S prime vaccination enhances CD4+ and CD8+ T cell responses**

330 Significantly higher percentages of CD4+ T-cells from SASA S > AdS+N group mice secreted
331 IFN-γ alone, IFN-γ and tumor necrosis factor-α (TNF-α), or IFN-γ, TNF-α, and interleukin-2 (IL-
332 2) as detected by intracellular cytokine staining (ICS) in response to S(wt) peptides as compared
333 to both the AdS+N or SASA S homologous groups (Fig. 5A, C, and D). Additionally, the mean
334 percentages were signficantly higher than that of the AdS+ N > SASA S group.

335 The enhancement of cytokine production by AdS+N boost of an SASA S prime was even
336 more pronounced for CD8+ T cells (Fig. 5B, D, and F). Cytokine production was significantly
337 higher in the SASA S > AdS+N group compared to both the homologous vaccination groups as
338 well as the AdS+N > SASA S group.

339 As expected, only T cells from mice receiving vaccination regimens that included delivery of
340 the N antigen by the AdS+N vaccine produced cytokines in response to N peptide stimulation.
341 Mean responses of both CD4+ and CD8+ T cells to N peptides were similar for groups receiving
342 AdS+N as a boost, either as part of homologous or heterologous vaccination (Figure 5A-F).

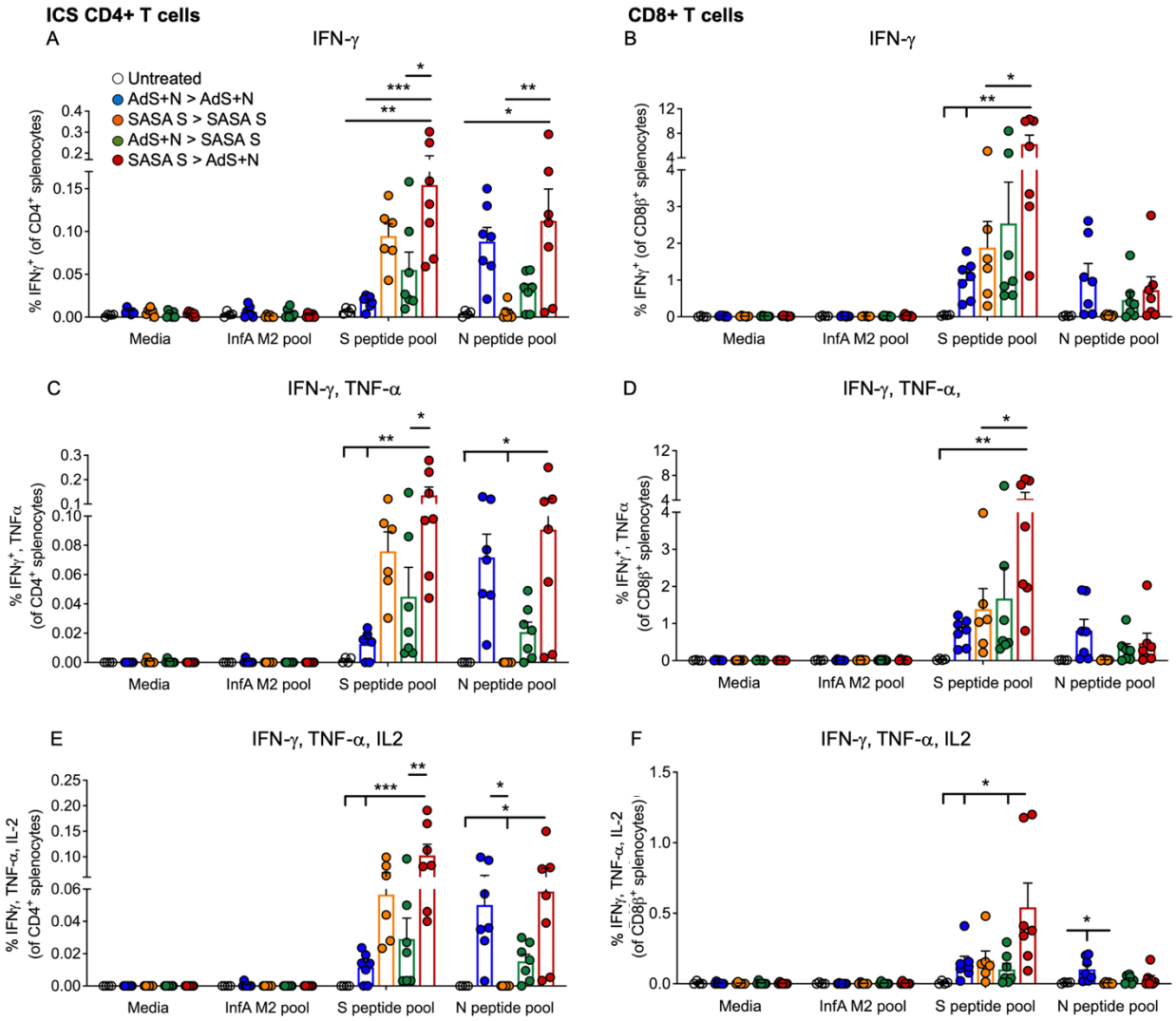

Fig. 5 *CD4+ and CD8+ T cell Intracellular cytokine staining (ICS) in response to S(wt) and N peptides*. (A, B) ICS for interferon-γ (IFN-γ), (C, D) IFN-γ and tumor necrosis factor-α (TNF-α), and (E, F) IFN-γ, TNF-α and interleukin-2 (IL-2) are shown for CD4+ and CD8+ T cells, respectively. Statistical analyses performed using one-way ANOVA and Tukey's post-hoc comparison of all groups to all other groups with the exception of comparison to the SASA S > SASA S group that did not receive an N antigen (comparisons to UnTx > UnTx are shown); where $*p \leq 0.05$, $**p < 0.01$, and $***p < 0.001$. Data graphed as the mean and SEM. The legend in A applies to all figure panels.

CD4+ and CD8+ T-cell production of IFN-γ was similar in response to either S(wt) or S(Delta) peptides

CD4+ and CD8+ T cells show similar levels of IFN-γ production in ICS in response to either S(wt) or S(Delta) sequence peptides (Fig. 6A and B, respectively). Patterns of CD4+ and CD8+

357 T-cell stimulation by S protein peptides between the vaccination regimens were also similar
358 between the S(wt) and S(Delta) peptides. Compared to the untreated control, the significance of
359 the increase in IFN-γ production was again the highest for the SASA S > AdS+N group for both
360 CD4+ and CD8+ T cells, and in response to either S(wt) or S(Delta) peptides.

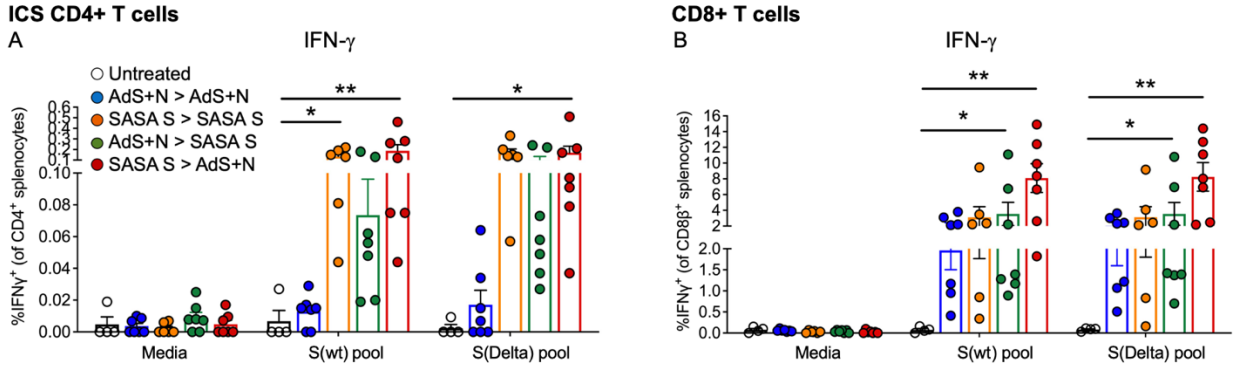

361
362 **Fig. 6** *CD4+ and CD8+ T-cell responses to S(wt) and S(Delta) peptides are similar*. Both CD4+
363 (A) and CD8+ (B) T cells show similar levels of interferon-γ (IFN-γ) production in ICS in response
364 to either S(wt) or S(Delta) sequence peptides. For both T-cell types, the greatest responses were
365 seen with SASA S > AdS+N vaccination. Statistical analyses performed using one-way ANOVA
366 and Tukey's post-hoc comparison of all groups to all other groups; where *p ≤ 0.05 and **p <
367 0.01. Data graphed as the mean and SEM. The legend in A applies to all figure panels.
368

369 **Numbers of IFN-γ-secreting splenocytes were the highest from mice receiving SASA S >**
370 **AdS+N heterologous vaccination**

371 As shown in Figure 7A, ELISpot detection of cytokine secretion in response to the S peptide
372 pool revealed that animals receiving heterologous SASA S > AdS+ N vaccination developed
373 significantly higher levels of S peptide-reactive IFN-γ-secreting T cells than all other groups
374 except the SASA S homologous group (which had a lower mean). Numbers of IFN-γ-secreting T
375 cells in response to the N peptide pool were similar for AdS+N homologous and SASA S > AdS+N
376 groups. T cells from SASA S > SASA S group animals did not secrete IFN-γ in response to the N
377 peptide pool, as expected, because the SASA S vaccine does not deliver the N antigen. While the
378 difference was not significant due to individual variation, the mean number of N-reactive

379 stimulated cells secreting IFN-γ due to AdS+N > SASA S vaccination was lower than the other
380 groups receiving a vaccine with N.

381 Induction of interleukin-4 (IL-4) secreting T cells was low for all animals in all groups (Fig.
382 7B), therefore the IFN-γ/IL-4 ratio was above 1 for all animals for which the ratio could be
383 calculated (Fig. 7C), reflecting the Th1-bias of all T-cell responses.

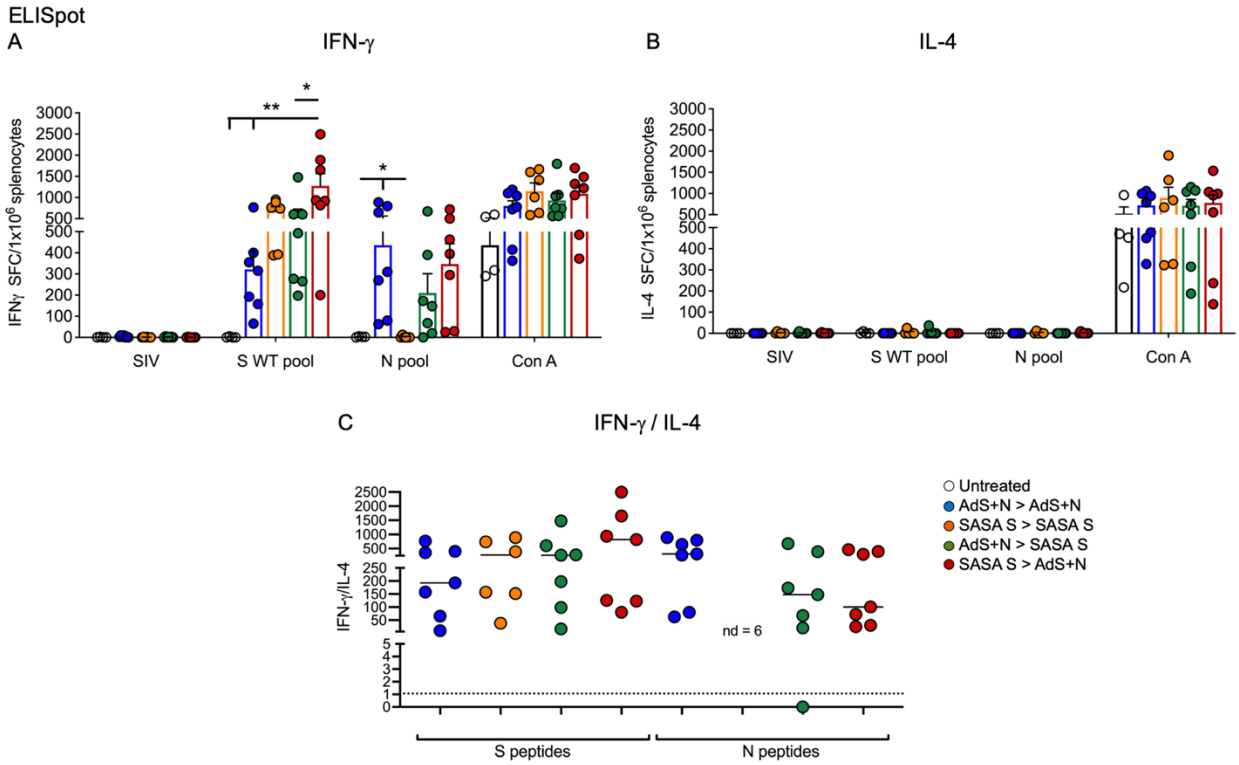

384
385 **Fig. 7** *Heterologous vaccination increases T-cell cytokine secretion in ELISpot*. (A) Numbers of
386 interferon-γ (IFN-γ) and (B) interleukin-4 (IL-4) secreting T cells in response to S WT and N
387 peptides pools. (C) The IFN-γ/IL-4 ratio; value of 1 indicated by dashed line. The ratio was not
388 determined (ND) for animals with very low IL-4 secretion. Statistical analyses performed using
389 one-way ANOVA and Tukey's post-hoc comparison of all groups to all other groups where *$p \leq$
390 0.05 and **$p < 0.01$. Data graphed as the mean and SEM. The legend in C applies to all figure
391 panels.
392
393 **Sera from mice receiving the SASA S vaccine neutralize Wuhan, Delta, and Beta**
394 **pseudoviruses**

395 Sera from the homologous SASA S group and both heterologously vaccinated groups
396 neutralized Wuhan (D614G), Delta (B.1.617.2), and Beta (B.1.351) pseudoviruses, as shown in

397 Figure 8. Sera from AdS+N homologous mice showed lower neutralization capability for all
398 strains. Neutralization of Wuhan strain pseudovirus by sera from SASA S homologous and SASA
399 S > AdS+N heterologous group mice was significantly greater than that from AdS+N > SASA S
400 mice, but there were no statistical differences among these 3 groups for the Delta or Beta strains.

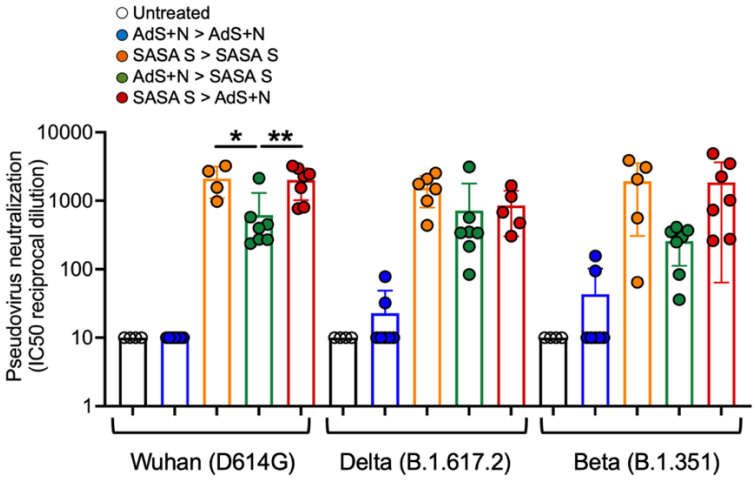

401
402 **Fig. 8** *Sera from SASA S > AdS+N heterologously vaccinated mice neutralizes Wuhan, Delta, and*
403 *Beta strain SARS-CoV-2 pseudovirus*. Neutralization of Wuhan strain pseudovirus by sera from
404 SASA S homologous and SASA S > AdS+N mice was significantly greater than that for AdS+N
405 > SASA S mice (as well as untreated and AdS+N homologous). There were no significant
406 differences between the SASA S homologous and the two heterologous groups for the Delta or
407 Beta strain pseudoviruses. Statistical comparison of IC50 values for untreated and AdS+N
408 homologous group mice with all/many values < the LOD was not performed. Statistical analyses
409 performed using one-way ANOVA and Tukey's post-hoc comparison of SASA S homologous,
410 AdS+N > SASA S, and SASA S > AdS+N groups to each other for each strain where *$p \leq 0.05$
411 and **$p < 0.01$; and for the same group for each different strain. Data graphed as the mean and
412 SEM.
413
414 **DISCUSSION**

415 The immune responses observed in the present study support our hypothesis that heterologous
416 vaccination provides an opportunity for increased humoral and cell-mediated responses. These
417 results and hypothesis are consistent with recently-published data supporting enhanced antibody
418 responses in patients who received heterologous vaccination with the currently-FDA authorized
419 COVID-19 vaccines. [35] Delivery of the SASA S vaccine elicited higher anti-S IgG than the AdS+N
420 vaccine, but the AdS+N vaccine provided the N antigen that broadened humoral responses and

421 thus the potential to enhance protection against future SARS-CoV-2 variants of concern that could
422 emerge. We note that mean anti-N IgG responses, while not statistically different among groups
423 that received the N antigen (not SASA S homologous) were, as predicted, highest with
424 homologous AdS+N vaccination.

425 Perhaps the most striking finding in the present study are the enhanced responses of S-specific
426 CD4+ and CD8+ T-cells in SASA S > AdS+N group mice, an effect that was most pronounced
427 for CD8+ T cells. The similarity of responses of CD4+ and CD8+ T cells to either S(wt) or S(Delta)
428 suggest this vaccine regimen has a high probability of conferring T-cell mediated protection
429 against the highly transmissible Delta variant in addition to humoral protection.

430 Immune responses elicited by SASA S > AdS+N vaccination were consistently the highest of
431 the groups tested (although not always significantly so) and we hypothesize that because the SASA
432 S vaccines elicits the greatest humoral response to S when given in any order – possibly reaching
433 the upper detection limit for our ELISA - it enhances CD4+ T-cell activation as these are closely
434 related to humoral/B cell responses. Therefore, CD4+ T-cell activation might be expected to be
435 higher after a boost if there are stronger pre-existing, prime-induced B cell responses, that is, when
436 SASA S is the prime. Adenovirus vectors such as that used for the AdS+N vaccine are good at
437 eliciting CD8+ T-cell responses, which we posit explains why CD8+ T-cell responses are only
438 slightly lower for homologous AdS+N vaccination (despite antibody and CD4+ T-cell responses
439 being lower), as compared to heterologous vaccination. CD8+ T-cell responses likely also benefit
440 from more robust pre-existing CD4+ T-cell and B cell responses, a condition that exists most
441 prominently when the SASA S vaccine is given as the prime. Effectively, enhanced CD4+-specific
442 T-helper responses seen with SASA S prime dosing might have provided conditions for the

443 enhanced CD8+ specific response upon AdS+N boost. The confirmation of this hypothesis awaits
444 further investigation.

445 Importantly, all of the vaccination regimens that included the SASA S vaccine neutralized
446 pseudovirus effectively, reflecting the strength of humoral responses to the SASA S vaccine. This
447 does not however indicate that the predominantly T-cell inducing AdS+N vaccine would not be
448 effective in an *in vivo* model of SARS-CoV-2 challenge; in fact, we have previously reported that
449 homologous AdS+N prime-boost vaccination of non-human primates confers protection against
450 viral challenge [6]. In the *in vivo* viral challenge testing paradigm, cell-mediated immunity (not
451 accessed in the pseudovirus assay) conferred by AdS+N vaccination likely plays a key role in
452 protection, as has been reported for natural infection of patients. [36-39]

453 The findings here, including cross-reactive humoral and T-cell responses to S Delta and - for
454 regimens including SASA S – neutralization of Wuhan, Delta, and Beta pseudovirus, support
455 ongoing studies of heterologous vaccination with the SASA S and AdS+N vaccines. Further
456 testing in pre-clinical models of SARS-CoV-2 challenge and clinical trials should be conducted to
457 assess the capability of this vaccine regimen to provide increased protection against COVID-19
458 and SARS-CoV-2 variants by combining the ability of SASA S to elicit vigorous humoral
459 responses with AdS+N's second, highly antigenic N antigen and T-cell response enhancement.

460

461

462

463

464

465

466 **REFERENCES**

467 1. Polack FP, Thomas SJ, Kitchin N, et al: Safety and Efficacy of the BNT162b2 mRNA
468 Covid-19 Vaccine. N Engl J Med 383:2603-2615, 2020
469 2. Ewer KJ, Barrett JR, Belij-Rammerstorfer S, et al: T cell and antibody responses
470 induced by a single dose of ChAdOx1 nCoV-19 (AZD1222) vaccine in a phase 1/2 clinical trial.
471 Nat Med 27:270-278, 2021
472 3. Shinde V, Bhikha S, Hoosain Z, et al: Efficacy of NVX-CoV2373 Covid-19 Vaccine
473 against the B.1.351 Variant. N Engl J Med 384:1899-1909, 2021
474 4. Sadoff J, Gray G, Vandebosch A, et al: Safety and Efficacy of Single-Dose
475 Ad26.COV2.S Vaccine against Covid-19. N Engl J Med 384:2187-2201, 2021
476 5. Voysey M, Clemens SAC, Madhi SA, et al: Safety and efficacy of the ChAdOx1
477 nCoV-19 vaccine (AZD1222) against SARS-CoV-2: an interim analysis of four randomised
478 controlled trials in Brazil, South Africa, and the UK. The Lancet 397:99-111, 2021
479 6. Gabitzsch E, Safrit JT, Verma M, et al: Dual-Antigen COVID-19 Vaccine
480 Subcutaneous Prime Delivery With Oral Boosts Protects NHP Against SARS-CoV-2 Challenge.
481 Front Immunol 12:10.3389/fimmu.2021.729837, 2021
482 7. Rice A, Verma M, Shin A, et al: Intranasal plus subcutaneous prime vaccination
483 with a dual antigen COVID-19 vaccine elicits T-cell and antibody responses in mice. Sci Rep
484 11:14917, 2021
485 8. Sieling P, King T, Wong R, et al: Prime hAd5 Spike plus Nucleocapsid Vaccination
486 Induces Ten-Fold Increases in Mean T-Cell Responses in Phase 1 Subjects that are Sustained
487 Against Spike Variants. medRxiv 2021.04.05.21254940, 2021
488 9. Niazi KR, Ochoa M-T, Sieling PA, et al: Activation of human CD4+ T cells by
489 targeting MHC class II epitopes to endosomal compartments using human CD1 tail sequences.
490 Immunology 122:522-531, 2007
491 10. Lin KY, Guarnieri FG, Staveley-O'Carroll KF, et al: Treatment of established
492 tumors with a novel vaccine that enhances major histocompatibility class II presentation of
493 tumor antigen. Cancer Res 56:21-6, 1996
494 11. Wu TC, Guarnieri FG, Staveley-O'Carroll KF, et al: Engineering an intracellular
495 pathway for major histocompatibility complex class II presentation of antigens. Proc Natl Acad
496 Sci USA 92:11671-5, 1995
497 12. Voigt EA, Gerhardt A, Hanson D, et al: A long-term thermostable self-amplifying
498 RNA vaccine against COVID-19. Manuscript in preparation, 2021
499 13. Spencer AJ, McKay PF, Belij-Rammerstorfer S, et al: Heterologous vaccination
500 regimens with self-amplifying RNA and adenoviral COVID vaccines induce robust immune
501 responses in mice. Nat Commun 12:2893, 2021
502 14. Wu L, Kong WP, Nabel GJ: Enhanced breadth of CD4 T-cell immunity by DNA
503 prime and adenovirus boost immunization to human immunodeficiency virus Env and Gag
504 immunogens. J Virol 79:8024-31, 2005
505 15. Casper C: New Technologies for Accessible, Durable and Broadly Protective
506 Coronavirus Vaccines IDRI http://www.idri.org/wp-content/uploads/2021/04/IDRI-
507 Technologies_Coronavirus.pdf:1-15, 2021

508 16. Erasmus JH, Khandhar AP, Guderian J, et al: A Nanostructured Lipid Carrier for
509 Delivery of a Replicating Viral RNA Provides Single, Low-Dose Protection against Zika. Mol Ther
510 26:2507-2522, 2018
511 17. Bloom K, van den Berg F, Arbuthnot P: Self-amplifying RNA vaccines for
512 infectious diseases. Gene therapy 28:117-129, 2021
513 18. Sandbrink JB, Shattock RJ: RNA Vaccines: A Suitable Platform for Tackling
514 Emerging Pandemics? Front Immunol 11:10.3389/fimmu.2020.608460, 2020
515 19. Zhang C, Maruggi G, Shan H, et al: Advances in mRNA Vaccines for Infectious
516 Diseases. Front Immunol 10:594, 2019
517 20. Zhang L, Jackson CB, Mou H, et al: SARS-CoV-2 spike-protein D614G mutation
518 increases virion spike density and infectivity. Nat Commun 11:6013, 2020
519 21. Weissman D, Alameh M-G, de Silva T, et al: D614G Spike Mutation Increases
520 SARS CoV-2 Susceptibility to Neutralization. Cell host & microbe 29:23-31.e4, 2021
521 22. Kirchdoerfer RN, Wang N, Pallesen J, et al: Stabilized coronavirus spikes are
522 resistant to conformational changes induced by receptor recognition or proteolysis. Sci Rep
523 8:15701-15701, 2018
524 23. Bangaru S, Ozorowski G, Turner HL, et al: Structural analysis of full-length SARS-
525 CoV-2 spike protein from an advanced vaccine candidate. Science 370:1089-1094, 2020
526 24. van Doremalen N, Lambe T, Spencer A, et al: ChAdOx1 nCoV-19 vaccine prevents
527 SARS-CoV-2 pneumonia in rhesus macaques. Nature 586:578-582, 2020
528 25. Zhu F-C, Li Y-H, Guan X-H, et al: Safety, tolerability, and immunogenicity of a
529 recombinant adenovirus type-5 vectored COVID-19 vaccine: a dose-escalation, open-label, non-
530 randomised, first-in-human trial. The Lancet 395:1845-1854
531 26. Amalfitano A, Begy CR, Chamberlain JS: Improved adenovirus packaging cell lines
532 to support the growth of replication-defective gene-delivery vectors. Proc Natl Acad Sci USA
533 93:3352-3356, 1996
534 27. Amalfitano A, Chamberlain JS: Isolation and characterization of packaging cell
535 lines that coexpress the adenovirus E1, DNA polymerase, and preterminal proteins: implications
536 for gene therapy. Gene Ther 4:258-63, 1997
537 28. Amalfitano A, Hauser MA, Hu H, et al: Production and Characterization of
538 Improved Adenovirus Vectors with the E1, E2b, and E3 Genes Deleted. J Virol 72:926, 1998
539 29. Seregin SS, Amalfitano A: Overcoming pre-existing adenovirus immunity by
540 genetic engineering of adenovirus-based vectors. Expert Opin Biol Ther 9:1521-31, 2009
541 30. Voigt EA, Fuerte-Stone J, Granger B, et al: Live-attenuated RNA hybrid vaccine
542 technology provides single-dose protection against Chikungunya virus. Mol Ther 29:2782-2793,
543 2021
544 31. Erasmus JH, Archer J, Fuerte-Stone J, et al: Intramuscular Delivery of Replicon
545 RNA Encoding ZIKV-117 Human Monoclonal Antibody Protects against Zika Virus Infection. Mol
546 Ther Methods Clin Dev 18:402-414, 2020
547 32. Gerhardt A, Voigt E, Archer M, et al: A Thermostable, Flexible RNA Vaccine
548 Delivery Platform for Pandemic Response. bioRxiv:2021.02.01.429283, 2021
549 33. Skordos I, Demeyer A, Beyaert R: Analysis of T cells in mouse lymphoid tissue and
550 blood with flow cytometry. STAR protocols 2:100351-100351, 2021

551 34. Crawford KHD, Eguia R, Dingens AS, et al: Protocol and Reagents for
552 Pseudotyping Lentiviral Particles with SARS-CoV-2 Spike Protein for Neutralization Assays.
553 Viruses 12:513, 2020
554 35. Atmar RL, Lyke KE, Deming ME, et al: Heterologous SARS-CoV-2 Booster
555 Vaccinations – Preliminary Report. medRxiv:2021.10.10.21264827, 2021
556 36. Grifoni A, Sidney J, Vita R, et al: SARS-CoV-2 human T cell epitopes: Adaptive
557 immune response against COVID-19. Cell Host Microbe 29:1076-1092, 2021
558 37. Tarke A, Sidney J, Kidd CK, et al: Comprehensive analysis of T cell
559 immunodominance and immunoprevalence of SARS-CoV-2 epitopes in COVID-19 cases. Cell Rep
560 Med 2:100204, 2021
561 38. Sekine T, Perez-Potti A, Rivera-Ballesteros O, et al: Robust T cell immunity in
562 convalescent individuals with asymptomatic or mild COVID-19. Cell 183:158, 2020
563 39. Tan AT, Linster M, Tan CW, et al: Early induction of functional SARS-CoV-2-
564 specific T cells associates with rapid viral clearance and mild disease in COVID-19 patients. Cell
565 Rep 34:108728, 2021
566